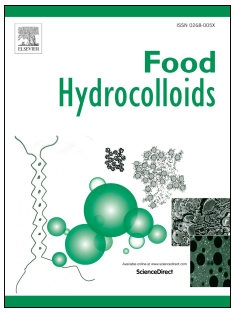

Dynamic adsorption and interfacial rheology of whey protein isolate at oil-water interfaces: effects of protein concentration, pH and heat treatment

Beibei Zhou, John T. Tobin, Stephan Drusch, Sean A. Hogan

PII: S0268-005X(21)00056-4

DOI: https://doi.org/10.1016/j.foodhyd.2021.106640

Reference: FOOHYD 106640

To appear in: *Food Hydrocolloids*

Received Date: 20 October 2020

Revised Date: 25 January 2021

Accepted Date: 27 January 2021

Please cite this article as: Zhou, B., Tobin, J.T., Drusch, S., Hogan, S.A., Dynamic adsorption and interfacial rheology of whey protein isolate at oil-water interfaces: effects of protein concentration, pH and heat treatment, *Food Hydrocolloids*, https://doi.org/10.1016/j.foodhyd.2021.106640.

Beibei Zhou: Conceptualization, Methodology, Investigation, Validation, Formal analysis, Data Curation, Writing - Original Draft, Visualization. **John T. Tobin:** Project administration, Funding acquisition. **Stephan Drusch:** Writing - Review & Editing, Supervision, Project administration. **Sean A. Hogan:** Conceptualization, Methodology, Writing - Review & Editing, Supervision, Project administration

Dynamic adsorption and interfacial rheology of whey protein isolate at oil-water interfaces: effects of protein concentration, pH and heat treatment

Beibei Zhou[a,b,*], John T. Tobin[a], Stephan Drusch[b], and Sean A. Hogan[a,*]

[a] Food Chemistry and Technology Department, Teagasc Food Research Centre, Moorepark, Fermoy, Co. Cork, Ireland, P61 C996

[b] Technische Universität Berlin, Department of Food Technology and Food Material Science, Königin-Luise-Str. 22, 14195, Berlin, Germany

E-mail addresses: beibei.zhou@teagasc.ie (B. Zhou), john.tobin@teagasc.ie (J.T. Tobin), stephan.drusch@tu-berlin.de (S. Drusch), sean.a.hogan@teagasc.ie (S.A. Hogan).

*: Corresponding authors:

Beibei Zhou

Teagasc Food Research Centre, Moorepark, Fermoy, Co. Cork, Ireland, P61 C996

Email address: beibei.zhou@teagasc.ie

Sean A. Hogan

Teagasc Food Research Centre, Moorepark, Fermoy, Co. Cork, Ireland, P61 C996

Email address: sean.a.hogan@teagasc.ie

Graphical abstract

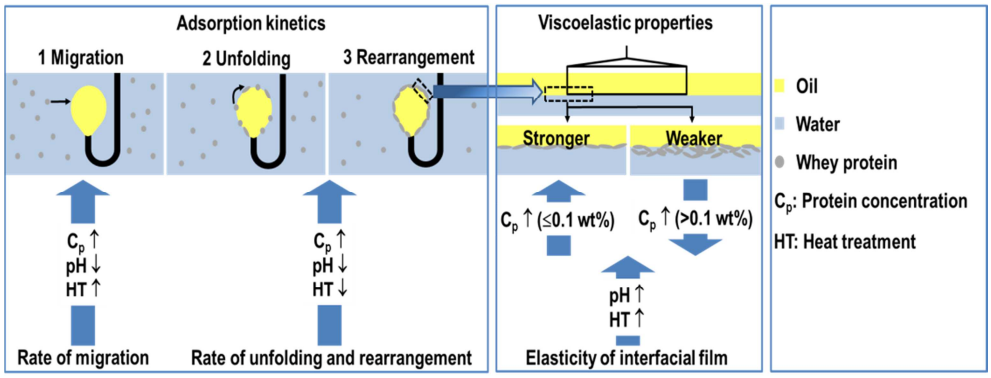

Dynamic adsorption and interfacial rheology of whey protein isolate at oil-water interfaces: effects of protein concentration, pH and heat treatment

Beibei Zhou[a,b,*], John T. Tobin[a], Stephan Drusch[b], and Sean A. Hogan[a,*]

[a] Food Chemistry and Technology Department, Teagasc Food Research Centre, Moorepark, Fermoy, Co. Cork, Ireland, P61 C996

[b] Technische Universität Berlin, Department of Food Technology and Food Material Science, Königin-Luise-Str. 22, 14195, Berlin, Germany

E-mail addresses: beibei.zhou@teagasc.ie (B. Zhou), john.tobin@teagasc.ie (J.T. Tobin), stephan.drusch@tu-berlin.de (S. Drusch), sean.a.hogan@teagasc.ie (S.A. Hogan).

*: Corresponding authors:

Beibei Zhou

Teagasc Food Research Centre, Moorepark, Fermoy, Co. Cork, Ireland, P61 C996

Email address: beibei.zhou@teagasc.ie

Sean A. Hogan

Teagasc Food Research Centre, Moorepark, Fermoy, Co. Cork, Ireland, P61 C996

Email address: sean.a.hogan@teagasc.ie

Abstract

The effects of bulk protein concentration, C_p, (0.01, 0.1, 1 wt%), pH (3, 4.7 and 7) and heat treatment (unheated or 95 °C for 30 min) on whey protein isolate (WPI) stabilized interfaces were examined. The interfacial pressure and shear rheology of WPI-stabilized sunflower oil-water (o/w) interfaces were characterized using a pendant drop tensiometer and a rheometer equipped with a Du Nöuy ring. The rate of WPI adsorption was faster at higer C_p and pH 3. Heat-enhanced surface activity was more pronounced at pH 7 compared to pH 3 as a result of greater heat stability of WPI at acidic pH. The elastic modulus of WPI stabilized interfaces increased with C_p (≤0.1 wt%). A further increase in C_p (to 1 wt%) resulted in monolayer collapse and weaker films. Non-heated (NHT) WPI formed less elastic interfacial films at pH 3 than at pH7. Heat treatment enhanced the elastic behavior of interfacial films with longer relaxation times. This may be associated with the formation of intermolecular β-sheets. The knowledge gained on the nature of WPI-stabilized interfaces can be used to better understand the stability of dairy emulsions during subsequent processing, digestion or storage.

Keywords

Oil/water interface

Whey protein isolate

Pendant drop tensiometry

Du Nöuy ring

Dynamic adsorption

Interfacial rheology

1. Introduction

Many emulsion-based food products are stabilized by amphiphilic proteins, which adsorb rapidly at thermodynamically unstable, immiscible interfaces (Amagliani & Schmitt, 2017; Dickinson, 1999). The surface activity of proteins can be determined by the time-dependent capacity of proteins to decrease the interfacial tension. During emulsification, adsorption of proteins with greater surface activity leads to more efficient reduction of interfacial tension, resulting in reduced energy input required to create new oil/water (o/w) interfaces (Amine, Dreher, Helgason, & Tadros, 2014; McClements, 2004). Upon adsorption, proteins unfold and rearrange at the interface to energetically more favorable conformations (Bos & van Vliet, 2001; Graham & Phillips, 1979b). Intermolecular interactions between proteins at the interface result in the formation of viscoelastic interfacial films, which contribute to emulsion stability (Kim, Cornec, & Narsimhan, 2005; Lam & Nickerson, 2013). During preparation and storage of emulsion-based food products, the conformation and intermolecular interactions of proteins are highly dependent on changes in environmental and processing conditions. Protein concentration (C_p), pH, ionic strength and heat-treatment, have considerable influence on adsorption behavior and mechanical properties of interfacial films (Roth, Murray, & Dickinson, 2000; Won et al., 2017). The kinetics of adsorption of proteins to o/w interfaces impact surface activity, which plays an important role in the formation of emulsion-based food products. Moreover, the mechanical strength of the interfacial film is directly related to the ability of emulsion droplets to withstand destabilizing processes such as coalescence, flocculation and Ostwald ripening (McClements & Jafari, 2018). Therefore, a comprehensive understanding of the effect of environmental and processing conditions on the interfacial properties of proteins is important for their use as

effective emulsifiers in food products (Dickinson, 1999; McClements, 2004; Wilde, Mackie, Husband, Gunning, & Morris, 2004).

Whey protein isolate (WPI) is widely used in food emulsions because of it's high nutritional quality and interfacial functionality (Deeth & Bansal, 2019; Schröder, Berton-Carabin, Venema, & Cornacchia, 2017). Individual whey proteins, in particular β-lactoglobulin, are commonly used as model proteins to study the adsorption dynamics and mechanical properties of interfacial films (Baldursdottir, Fullerton, Nielsen, & Jorgensen, 2010; Beverung, Radke, & Blanch, 1999; Cornec, Cho, & Narsimhan, 1999; Cornec, Kim, & Narsimhan, 2001; Kim et al., 2005; Roth et al., 2000; Schestkowa et al., 2019; Tang & Shen, 2015; Wierenga, Egmond, Voragen, & de Jongh, 2006; Won et al., 2017). However, individual whey protein species exhibit different interfacial properties under various environmental conditions. For instance, β-lactoglobulin is reported to be more surface active than α-lactalbumin at low protein concentrations, whereas little difference in surface activity has been found between them at high concentrations. In both cases, BSA is the least surface active of the whey proteins (Paulsson & Dejmek, 1992). The diffusion and unfolding properties of α-lactalbumin are faster than ß-lactoglobulin (Cornec et al., 1999). Furthermore, adsorption and unfolding of α-lactalbumin are faster at acidic compared to neutral pH (Cornec et al., 2001) while ß-lactoglobulin adsorbs faster at basic pH than neutral pH (Schestkowa et al., 2019). ß-lactoglobulin and BSA exhibit maximum interfacial shear elastic moduli around pI, which has been associated with reduction in surface charge and decreasing electrostatic repulsion between proteins (Kim & Kinsella, 1985; Roth et al., 2000).

The interfacial behavior of protein mixtures (in WPI) may not be readily inferred from single-protein, model systems (Marinova et al., 2009). The differing surface activities

of individual whey proteins make predictions of WPI interfacial behavior challenging. It has been reported that WPI exhibited the most rapid decline in surface tension and greatest surface dilatational elasticity, at a pH close to its pI, compared to pH 3 and 7 (Davis, Foegeding, & Hansen, 2004). This study focused on the air/water interface and short-term interfacial rheological properties, which is relevant to foam formation. Moreover, in a study on the activity of WPI at the o/w interface, Lam and Nickerson (2015) reported similar trends and correlated this behavior to increased protein aggregate size (due to minima surface charge at pI). However, this study did not address the influence of pH-induced preferential adsorption of individual whey proteins on the surface activity and mechanical properties of WPI adsorbed interfaces. In the case of mixtures of α-lactalbumin and ß-lactoglobulin, protein adsorption appears to be proportional to their concentration at pH 7, while more α-lactalbumin adsorbs at pH 3 (Hunt & Dalgleish, 1994). Preferential adsorption, induced by pH, leads to changes in interfacial protein composition, which also impacts the mechanical properties of interfacial films. Studies showed that ß-lactoglobulin is more surface active at pH 7 than pH 3, whereas α-lactalbumin is more surface active at pH 3 than pH 7 (Buchmann et al., 2019; Cornec et al., 2001; Gao et al., 2008; Lech, Delahaije, Meinders, Gruppen, & Wierenga, 2016). Therefore, although ß-lactoglobulin is the major protein in WPI, the interfacial properties of WPI are not necessarily determined exclusively by ß-lactoglobulin.

Some controversy exists on findings related to the interfacial properties of heat-treated whey proteins. It has been observed by some researchers, at o/w interfaces, that heat-treatment lead to an increase in adsorption rate with higher interfacial modulus (Kim et al., 2005; Rodríguez Patino, Rodríguez Niño, & Sánchez, 1999). In contrast, others have found reduced rates of adsorption and either only minor

changes or decrease in modulus values for heat-treated whey proteins (Davis & Foegeding, 2004; Roth et al., 2000; Yang, Thielen, Berton-Carabin, van der Linden, & Sagis, 2020). These differences may be due to differences in the susceptibility to denaturation of individual whey proteins under a variety of heat treatment conditions. When heated at ≤90 °C, α-lactalbumin undergoes reversible denaturation but becomes irreversibly denatured at >90 °C (Boye, Alli, & Ismail, 1997; Chaplin & Lyster, 2009; McGuffey, Epting, Kelly, & Foegeding, 2005). In contrast, ß-lactoglobulin has been found to be irreversibly denatured at or around it's denaturation temperature (Arnebrant, Barton, & Nylander, 1987). Although the former study associates the interfacial properties with increased surface hydrophobicity due to general alteration of protein structure, there is still insufficient information on the heat-induced changes to secondary structure and associated effects on interfacial properties.

It has been reported that bulk protein concentration impacts protein structure at the interfaces and the thickness of interfacial films (Graham & Phillips, 1979b). Recently, researchers have examined the critical interfacial concentration (CIC), at which full monolayer coverage is achieved. At protein concentrations above the CIC, multilayers begin to form (Schestkowa, Drusch, & Wagemans, 2020; Tamm, Sauer, Scampicchio, & Drusch, 2012). The CIC for WPI has been determined to lie in the range from 0.10-0.13 wt% (Tamm et al., 2012). In order to gain a comprehensive understanding of the influence of interfacial protein structures as well as the thickness of interfacial films on interfacial functionality, the effect of protein concentrations on the interfacial viscoelastic properties, outside this range should also be considered.

147 The aim of this work is to study, in a systematic way, the effect of C_p, pH and heat-
148 treatment on the dynamics of adsorption and the interfacial rheological properties of
149 WPI at o/w interfaces. For this purpose, the dynamic interfacial tension and protein
150 adsorption kinetics of WPI at pH 3 and 7 were analyzed by pendant drop tensiometry
151 at concentrations from 0.01 to 1 wt%. In order to minimize the influence of partial or
152 reversible denaturation of α-lactalbumin and β-lactoglobulin, WPI was heated at
153 95 °C for 30 min (HT WPI) and compared with non-heated (NHT) WPI. Changes to
154 the secondary structures of proteins were characterized using FTIR. Viscoelastic
155 properties of interfacial films were analyzed using a rheometer equipped with a Du
156 Noüy ring. In order to determine the influence of pH-induced preferential adsorption
157 and surface charge, the interfacial rheological properties of α-lactalbumin, β-
158 lactoglobulin and WPI were analyzed at pH 3, 4.7 and 7.
159

160 **2. Materials and methods**

161 2.1. Materials

162 Whey protein isolate (WPI) Bipro® was supplied by Davisco Foods International
163 (Eden Prairie, Minnesota, U.S.A.) and had the following composition: 91.4 ± 0.2 wt%
164 protein, 0.2 ± 0.01 wt% fat, 1.3 ±0.4 % ash and 6.1 ± 0.01 wt% moisture. α-
165 lactalbumin and β-lactoglobulin were obtained from Sigma Aldrich (St. Louis,
166 Missouri, U.S.A.). Sunflower oil was purchased from a local supermarket. Citric acid
167 ($C_6H_8O_7$), di-Sodium hydrogen phosphate anhydrous (Na_2HPO_4) and Florisil, 60-100
168 mesh were obtained from Sigma Aldrich (Arklow, Ireland.) All solutions used were
169 prepared in ultrapure Milli-Q water.
170

171 2.2. Oil purification

To remove any surface active impurities, sunflower oil was mixed with Florisil at a ratio 5:1 (w/w) and stirred at room temperature at 500 rpm for 2 h. The mixture was then centrifuged at 10,000 x g for 20 min to remove the Florisil. To verify the purity of the sunflower oil, it's interfacial tension was determined against Milli-Q water using a pendant drop tensiometer (Attention Theta tensiometer, Biolin Scientific, Finland) for 1 h. This procedure was repeated until no significant change of the interfacial tension was determined. The equilibrium interfacial tension attained at the interface between purified sunflower oil and Milli-Q water was 36.5 mN/m.

2.3. Sample preparation

Proteins were dispersed in 20 mM Na_2HPO_4/citric acid buffer solutions to the desired concentrations (0.01, 0.1 or 1 wt% protein) at pH 3, 4.7 or 7. Heat-treated solutions were prepared by heating in a water bath at 95 °C for 30 min, and cooled immediately in ice slurry to room temperature, prior to further analysis. No visible aggregation or precipitation of WPI was observed following heat-treatment.

2.4. ζ-potential and particle size analysis

ζ-potential and particle size were determined by dynamic light scattering (DLS) Zetasizer Nano ZS (Malvern Instruments, Malvern, Worcestershire, U.K.) with a 4 mW helium-neon laser. For ζ-potential measurements, approximate 1mL of sample was slowly injected into the folded capillary cell. Six measurements were conducted for each sample at voltages between 50 and 150 mV. The ζ-potential was calculated from the electrophoretic mobility data using the Smoluchowski model. For particle size measurements, all samples were equilibrated in disposable polystyrene cuvettes at 21 °C for 120 s. Measurements were performed using refractive indices

of 1.45 and 1.33 for proteins and buffer, respectively, at backscattering angle of 173° and wavelength of 633 nm.

2.5. Fourier transform infrared spectroscopy

Infrared adsorption spectra of protein solutions were measured against water, as background, by FTIR spectroscopy (Bruker Tensor 27, Bruker Optik GmbH, Germany) equipped with a thermally controlled BioATR cell II. Sample solutions (20 μL) were loaded into the well of the sample cell and infrared adsorption spectra collected from 400−4000 cm^{-1}. Each spectrum was an average of 120 scans at a resolution of 4 cm^{-1}. All experiments were conducted in triplicate. Atmospheric corrections (H_2O and CO_2 compensations), vector normalization, and second derivative functions of the amide I region (1700−1600 cm^{-1}) were conducted using OPUS 7.5 software (Bruker Optik GmbH, Germany). The spectral region was fitted with Gaussian band profiles using Origin 2019b software (OriginLab Corp., Northampton, MA, USA) and the area of each band was expressed as a percentage of the total according to the protocol of (Yang, Yang, Kong, Dong, & Yu, 2015)

2.6. Interfacial adsorption

The adsorption process for proteins at the o/w interface has been condensed into three steps: (i), migration of bulk proteins to the interface, (ii), adsorption (penetration) and unfolding of proteins at the interface, and (iii), rearrangement of adsorbed protein layer towards more energetically favorable conformations (Graham & Phillips, 1979b). The adsorption kinetics of WPI at the o/w interface can be monitored by measuring changes in interfacial pressure (π) (Rodríguez Patino et al., 1999), where π is defined as the change in interfacial tension of a protein-stabilized interface

compared to a pure o/w interface. It can be expressed as $\pi = \gamma_0 - \gamma$, where γ_0 is the interfacial tension of the pure o/w interface and γ is the interfacial tension of the protein adsorbed interface. Interfacial tension was measured using a pendant drop tensiometer (Attention Theta tensiometer, Biolin Scientific, Finland). A droplet of oil, with a volume of 10 μL, was formed at the tip of a stainless-steel, hooked needle (gauge 22) immersed in the WPI solution within a glass cuvette. The shape of the oil droplet was recorded continuously by a high-speed camera for 15000 s with a frame rate of approx. 84 frames per minute for the first 5 min and 3 frames per minute for the following 245 min. Interfacial tension was calculated by fitting the Young-Laplace equation to the drop shape, using One Attention software (Biolin Scientific, Finland).

The initial step of protein adsorption can be described by the Ward and Tordai model (Graham & Phillips, 1979a; Ward & Tordai, 1946) (Eq 1).

$$\pi = 2C_0KT\left(\frac{Dt}{3.14}\right)^{1/2} \quad (1)$$

where C_0 is the protein concentration in the bulk solution, K is the Boltzmann constant and T is the absolute temperature, D is the diffusion coefficient and t is the time. This model is based on the following assumptions: the migration of proteins to the interface is diffusion-controlled; no energy barriers to adsorption exist during migration; the conformation of proteins does not change after adsorption (Guzey, McClements, & Weiss, 2003). Therefore, good linear fits of π plotted against $t^{1/2}$ can only be obtained when the interfacial pressure is low ($\pi < 10$ mN/m). The slope of this linear region signifies the rate of initial diffusion-controlled migration (k_{diff}) (Álvarez Gómez & Rodríguez Patino, 2006; Rodríguez Niño, Sánchez, Ruíz-Henestrosa, & Rodríguez Patino, 2005; Rodríguez Patino et al., 1999). However, the migration of proteins to the interface is influenced, not only by the diffusion of proteins to the interface, but also by convection due to flow conditions during initial

246 formation of the oil droplet (Wahlgren & Elofsson, 1997). Given that the droplets
247 were formed at a constant flow rate, any convection-induced differences between
248 samples can be neglected.
249 After migration of proteins to the interface, the rate of penetration, unfolding and
250 conformational rearrangements of WPI can be monitored by a first-order equation
251 (Baeza, Carrera Sanchez, Pilosof, & Rodríguez Patino, 2005; Perez, Sánchez,
252 Patino, Rubiolo, & Santiago, 2010; Rodríguez Patino et al., 2007) (Eq 2).
253

$$\ln \frac{\pi_{15000} - \pi_t}{\pi_{15000} - \pi_0} = -k_i t \quad (2)$$

254 where π_0, π_t and π_{15000} are the interfacial pressures at time 0, at any experimental
255 time point and at the final adsorption time point (15000 s), respectively. k_i is the first-
256 order rate constant. A plot of ln[(π15000 – πt) / (π15000 – π0)] as a function of time
257 normally yields two linear regions. The first slop is taken to correspond to a first-
258 order rate constant of penetration and unfolding (k_u) while the second slop is taken
259 as a first-order rate constant of rearrangement (k_r).
260

261 2.7. Interfacial shear rheology

262 Measurements of the interfacial rheology of proteins were carried out using a control-
263 stress rheometer (AR G2 Rheometer, TA Instruments, Crawley, UK) equipped with a
264 Du Noüy ring geometry (platinum ring with diameter 19.3 mm and wire diameter 0.36
265 mm) as described by Wang et al. (2012) (Wang, Xie, et al., 2012). The signals of
266 oscillation stress and strain are calculated from the raw signals of torque and angular
267 displacement, respectively. The Boussinesq number (Eq. 3) is a dimensionless
268 number used to describe the ratio of the interfacial drag to the bulk drag experience
269 by the geometry.

$$N_{Bq} = \frac{\eta_s}{(\eta_1 + \eta_2)l} \quad (3)$$

Where η_s is the interfacial viscosity, η_1 is the oil viscosity, η_2 is the protein solution viscosity, l is the characteristic length scale, which is related to the ratio of the contact area between the geometry and the bulk phases to the perimeter of the geometry in contact with the interface (Derkach, Krägel, & Miller, 2009; Vandebril, Franck, Fuller, Moldenaers, & Vermant, 2010). The N_{Bq} was much larger than 1 for the protein systems examined in this study, indicating that the interfacial stress dominated the bulk parameters and that the contribution of the bulk phases can be neglected (Yang et al., 2020).

A cone geometry was used to zero the gap in order to avoid damage to the ring. 10 mL protein solution was placed in a 50 mm diameter glass beaker and the ring was lowered to make contact with the surface. 10 mL sunflower oil was carefully loaded on top of the protein solution, by trickling down the side of the beaker, using a transfer pipette. Oscillatory shear measurements were performed according to the method of Baldursdottir et al. (Baldursdottir et al., 2010). Dynamic time sweeps were conducted at a constant strain amplitude of 0.1% (i.e. within the linear viscoelastic region) and a constant frequency of 0.1 Hz for 60 min. Dynamic frequency sweeps were performed between 0.02 and 1 Hz at a constant strain amplitude of 0.1%. Dynamic strain sweeps were carried out in the range of 0.05-100% at a constant frequency of 0.1 Hz.

2.8. Statistical analysis

Experiments were performed in triplicate, meaning three separate protein solutions and/or o/w systems were prepared for analysis. Statistical analyses were performed

by one-way ANOVA with a least significant difference (LSD) test, using IBM SPSS Statistics for Windows, version 26 (IBM Corp., Armonk, N.Y., USA) to determine the significance of differences ($p \leq 0.05$).

3. Results and discussion

3.1. Particle size and ζ-potential

The ζ-potential of WPI solutions differed significantly as a function of pH. ζ-potential ranged from 27.1 ± 3.2 mV at pH 3, to -0.1 ± 0.5 mV at pH 4.7 and -21.1 ± 1.1 mV at pH 7. Particle size distributions of NHT WPI were between 2 and 10 nm with peak values around 3 nm at pH 3 and 5 nm at pH 7 (Figure 1). ß-lactoglobulin exists essentially in the monomeric form at < pH 3.5 and is predominantly a dimer in the pH range between 5.5 and 7.5 (Fox, 2008). Therefore, the higher peak values at pH 7 may be due to dimerization of ß-lactoglobulin. HT WPI at pH 7 showed wider size distributions (4-50 nm) with peak values at around 10 nm, which was presumably the result of heat-induced aggregation. However, as a consequence of increased thermostability of ß-lactoglobulin at acidic pH (deWit & Klarenbeek, 1984), only a slight increase in the average peak value was observed in HT WPI at pH 3, indicating the formation of irreversibly unfolded monomers (Harwalkar, 1980).

3.2. FTIR analysis

The amide I region (1700-1600 cm^{-1}) is associated primarily with stretching vibrations of C=O bonds and is sensitive to changes in the secondary structures of proteins (Allain, Paquin, & Subirade, 1999). Second derivative curves from FTIR spectra of WPI before and after heating at different pH values are shown in Figure 2. From the second derivative spectrum, 5-6 peaks per curve can be observed for 5 main secondary structures of WPI. The peaks at 1610-1620 cm^{-1} are indicative of

intermolecular β-sheet structures (Lu et al., 2015), while peaks at 1627-1630 cm^{-1}, 1631-1635 and 1689-1693 have been assigned to intramolecular β-sheet structures (Murphy, Fenelon, Roos, & Hogan, 2014; Yang et al., 2015). The characteristic peaks for random coil and α-helix conformation are located at 1644-1650 cm^{-1} and 1654-1660 cm^{-1} respectively (Barreto, Elzinga, & Alleoni, 2020; Yang et al., 2015). Peaks at 1674-1676 cm^{-1}, 1678-1682 cm^{-1} and 1683-1687 cm^{-1} are associated with β-turn structures (Chou & Fasman, 1977).

In order to better understand the changes to amide I protein components under different environmental and process conditions, curve fitting was used to determine the relative proportions of secondary structural features (Table 1 and Figure 3). The band associated with α-helix structure had greater intensity in NHT WPI prepared at pH 3 (34 ± 1%) compared to pH 7 (27 ± 2%). According to Zhai, Day, Aguilar and Wooster (2013), α-helix is the most compact amphipathic conformation and adsorbs preferentially at the oil/water interface. Heat treatment resulted in significant losses of intramolecular β-sheet structure (from 47 ± 1% to 35 ± 1%) and formation of intermolecular β-sheets (1 ± 1% to 7 ± 1%) at pH 3. Meanwhile, for WPI at pH 7, intermolecular β-sheet structure was absent in NHT WPI (0%) but increased to 11 ± 2% in HT WPI, at the expense of intramolecular β-sheets (from 42 ± 2% to 31 ± 2%). This is comparable to the observations of earlier studies (Kehoe, Remondetto, Subirade, Morris, & Brodkorb, 2008; Krebs, Devlin, & Donald, 2006) . A significant reduction in α-helix conformation from 27 ± 2% to 20 ± 1% was also observed for WPI after heating at pH 7.

3.3. Interfacial pressure isotherm of WPI

Interfacial pressure (π) increased with time irrespective of pH and/or heat treatment (Figure 4), which is in good agreement with previous findings (Perez, Carrara,

Sánchez, Santiago, & Rodríguez Patino, 2009; Rodríguez Niño et al., 2005; Rodríguez Patino et al., 1999). The rate of increase in π decreased with time, which is also supported by Graham and Phillips (1979a) and Álvarez Gómez and Rodríguez Patino (2006), who attributed it to surface saturation by proteins and increased electrostatic energy barriers to further adsorption.

The magnitude of $\pi_{15,000}$ was generally greater at higher C_p (Figure 5). It can be observed that, almost without exception, HT WPI had significantly higher $\pi_{15,000}$ than NHT protein and that WPI became more surface active following heat treatment. This is likely the result of unfolding of globular proteins (and exposure of hydrophobic moieties) during heat treatment. According to Cao, Xiong, Cao and True (2018) and Rodríguez Patino et al. (1999), surface activity of heat-treated proteins was consistent with reported changes in surface hydrophobicity. The enhancement of surface activity by heat treatment was less pronounced at pH 3 than pH 7, which may be due to greater heat stability at low pH. Most α-helix secondary structures were retained in WPI heated at pH 3 (Figure 2, Table 1). This consequently led to less extensive increases in surface hydrophobicity for whey proteins heated at low pH (Chandrapala et al., 2015).

3.3.1. Migration to the o/w interface

The first step of the protein adsorption process involves migration of proteins from the bulk phase to the o/w interface. The rate of diffusion-controlled migration can be characterized by applying Eq. 1 to the plots of interfacial pressure versus the square root of time. For the purposes of clarity, two examples of the plots of π against $t^{1/2}$ are shown in Figure 4. It should be noted that discussion of the adsorption kinetics of WPI refers to the overall behavior of a number of whey protein species, which will be

presented, for the convenience of the reader, as 'WPI'. The characteristic parameters derived from these plots for the diffusion of NHT and HT WPI are summarized in Table 2. At C_p >0.1 wt%, the migration step for WPI became too fast to be detected with the tensiometry method used in this study. Thus, the slope of the initial jump of π-$t^{1/2}$ is used as an estimation of the rate of initial diffusion-controlled migration, k_{diff} (Table 2). The results for 1 wt% NHT and HT WPI at pH 3, at C_p of 0.1-1 wt%, are not included in Table 2, because the initial values of π were > 10 mN/m.

The adsorption process of WPI at relatively short adsorption times (within the timescale of these experiments), i.e. up to about 47.8 s was controlled by diffusion of protein from the bulk phase to the interface. This diffusion-controlled period, t_{diff} became extended at lower C_p (Table 2). The values for k_{diff} in NHT WPI were dependent on the C_p in the bulk phase. It can be observed that k_{diff} values increased with C_p at both pH 3 and 7 (Table 2). This suggests that the concentration gradient is the driving force for diffusion of WPI, an observation supported by previous results for WPI o/w interfaces at pH 5 (Rodríguez Patino et al., 1999) and BSA at o/w interfaces at pH 7 (Tang & Shen, 2015).

The concentration gradient is, however, not the only the driving force for diffusion and adsorption. A chemical potential gradient from interactions of the interface with the hydrophobic, electrostatic, hydration and conformational potentials of proteins also acts as driving force (Doelle, Rokem, & Berovic, 2009). The k_{diff} of NHT WPI is higher at pH 3 with a shorter diffusion-controlled period compared to pH 7 (Table 2). β-lactoglobulin exists in a dynamic, monomer-dimer equilibrium under various pH conditions. The dimeric form is predominant at neutral pH and is driven mainly by hydrophobic forces (Mercadante et al., 2012). The monomeric form of β-lactoglobulin

396 is dominant at pH 3 as a result of dimer dissociation (Sakurai & Goto, 2002), which
397 exposes more hydrophobic sites (Liu, 2009; Martinez & Pilosof, 2018). It appears
398 from this study that increased hydrophobicity under acidic conditions promoted a
399 shorter diffusion period. At both pH values, HT WPI appeared to migrate more
400 rapidly than NHT samples (Table 2). The mechanism of denaturation and
401 aggregations of whey proteins has been described as a multistep process by
402 Mulvihill and Donovan (1987) and Wijayanti, Bansal and Deeth (2014). During the
403 initial step of heat treatment, the monomer-dimer equilibrium of β-lactoglobulin is
404 shifted toward the monomeric state. With increasing temperature, monomers unfold
405 with exposure of the free thiol group (normally buried within the the hydrophobic
406 core). Some of the denatured monomers are then involved in irreversible
407 aggregation reactions. In a generalized scheme, this reaction results in formation of
408 two types of aggregates: smaller ones held together, primarily, by disulfide (covalent)
409 bonds formed via thiol group oxidation and/or thiol-disulfide interchange reactions,
410 and larger aggregates with further involvement of non-covalent interactions.
411 Depending on the extent of heat treatment, denatured monomers of β-lactoglobulin
412 can coexist with such aggregates (Croguennec, O'Kennedy, & Mehra, 2004).
413 According to the Stokes-Einstein diffusion model, the diffusion coefficient is inversely
414 proportional to the cubic root of molecular size (Rodríguez Patino et al., 2007; Ruíz-
415 Henestrosa et al., 2007; Yu et al., 2019). It can be inferred that the aggregates in HT
416 WPI diffuse more slowly than native proteins due to their larger particle size (Figure
417 1). However, denatured monomers remaining in HT WPI, with increased exposure of
418 previously buried hydrophobic amino acids, may result in faster diffusion compared
419 to NHT WPI (Mahmoudi, Axelos, & Riaublanc, 2011; Wang, Xia, et al., 2012). This

observation is supported by previous studies on WPI and ß-lactoglobulin at the o/w interface (Kim et al., 2005; Rodríguez Patino et al., 1999).

The increase in k_{diff} values observed for HT WPI at pH 3 was less pronounced. It may be that the increase in surface hydrophobicity and protein flexibility following heating was less extensive under acidic conditions. It has been reported that the conformation of WPI is more rigid and resistant to denaturation at pH 3 than at pH 7 (Shimizu, Saito, & Yamauchi, 1985). According to Kella and Kinsella (1988), enhanced heat stability at acidic pH could be due to additional hydrogen bonding as a result of protonation of carboxyl groups in proteins and the loss of localized electrostatic interactions of the ionized carboxylates.

3.3.2. Penetration (adsorption), unfolding and re-arrangement of protein at the interface

After the migration period, the rate of adsorption gradually decreases. This has been attributed to an energy barrier generated by penetration, unfolding and conformational rearrangements of adsorbed protein at the interface (Cornec et al., 1999; Graham & Phillips, 1979a; Rodríguez Patino et al., 1999).

The rate constants of penetration, unfolding and re-arrangement steps derived from Figure 6 are collated in Table 3. In general, the rate constant of penetration and unfolding, k_u increased with C_p for NHT WPI at both pH 3 and 7. The penetration and unfolding of proteins at the interface is facilitated at higher C_p, due to the concentration gradient effect, an effect supported by previous observations for BSA at an o/w interface (Tang & Shen, 2015). In all cases, the magnitude of k_u and the rate constant of rearrangement, $k_{r,}$ was higher for NHT than HT samples. This observation might be associated with the formation of protein aggregates (Figure 1)

445 in which hydrophobic moieties are no longer available for surface interactions due to
446 their involvement in protein-protein associations. It is believed that protein
447 aggregates are more thermodynamically stable with lower free energy than the
448 native folded state (Baldwin et al., 2011; Jahn & Radford, 2008). A similar
449 dependence of k_r on heat treatment has been observed in soy glycinin nanoparticles
450 at the o/w interface (Liu & Tang, 2016). The values of k_u were also higher at pH 3
451 compared to pH 7, indicating that WPI penetrated and unfolded faster under acidic
452 conditions. This may be attributed to increased surface hydrophobicity as a result of
453 dimer dissociation (Liu, 2009). Shimizu et al. (1985), using hydrophobic
454 chromatography and fluorescent probe methodologies, reported significantly higher
455 relative surface hydrophobicity values for β-lactoglobulin at pH 3 than at pH 7. The
456 dependence on pH for the competitive adsorption of α-lactalbumin and β-
457 lactoglobulin could also be a possible cause for the increase in k_u at low pH. Hunt
458 and Dalgleish (1994) reported that the interfacial layer at pH 3 contains much higher
459 levels of α-lactalbumin than β-lactoglobulin, whereas the opposite was observed at
460 pH 7. The rate of unfolding of α-lactalbumin was also found to be much more rapid
461 than for β-lactoglobulin (Cornec et al., 1999), which may facilitate faster unfolding of
462 WPI at acidic pH. Furthermore, secondary structural changes to whey proteins at pH
463 3 exhibited a higher proportion of α-helices than at pH 7 (Figure 2), which is thought
464 to adsorb preferentially at the oil/water interface (Zhai et al., 2013).
465
466 *3.4. Interfacial rheology of WPI adsorbed films*
467 Interfacial shear rheology characterizes the viscoelastic properties of the interface
468 under shear deformation. To trace the development of intermolecular protein
469 interactions and the mechanical strength of the interfacial layer, time sweeps were

performed at a constant frequency of 0.1 Hz and a constant strain amplitude of 0.1%. This amplitude ensured that measurements were made within the linear viscoelastic region in order to avoid damage to interfacial structures. The interfacial elastic (G′) and viscous moduli (G″) of adsorbed WPI protein layers are shown in Figure 7. It can be seen that interfacial moduli generally increased with time, which is indicative of increased protein-protein interactions emanating from protein unfolding and rearrangements at the interface (Langevin, 2014). At pH 7, the growth rate of G′ increases with C_p (Figure 7 c), which is comparable to the behavior of BSA at an o/w interface (Baldursdottir et al., 2010). At 1 wt% WPI, at pH 7, elastic moduli, increased and attained a maximum during the first 30 minutes, before subsequently decreasing with time (Figure 7 c). A similar phenomenon has also been observed for ß-casein at the interface, which was attributed to the possibility that subsequently adsorbed proteins are hindered (sterically) from attaining optimal protein conformation at higher concentrations (Wüstneck et al., 2012).

G′ values after adsorption for 3600s (G'_{3600}) increased as C_p increased from 0.01 to 0.1 wt% (Figure 7 c). A further increase in bulk C_p (to 1 wt%) resulted in a slight reduction in G'_{3600}, suggesting that the highest C_p did not necessarily result in the 'strongest' interfacial structure. Graham and Phillips (1980) also reported a decrease in G′ at higher concentrations. Furthermore, the apparently weaker interfacial structures formed at 1 wt% WPI as further confirmed by the strain sweep data shown in Figure 8. WPI stabilised interfaces show a linear viscoelastic region (LVR) up to a critical strain amplitude of 0.4%. In the case of WPI pH 7, G′ values were higher than G″ within the LVR but started to decrease with increasing strain amplitude above this critical strain (interfacial yield strain). This reflects a breakdown in the network structure of the interfacial film. The strain value for the G′-G″ crossover point, above

which the interfacial film became predominantly viscous in nature, was lowest at 1 wt% WPI. This suggests that interfacial stability is not necessarily promoted by protein concentration. According to Schestkowa et al. (2020), the critical interfacial concentration (CIC), at which the interface is fully covered by protein was determined to be 0.2-0.31 wt%. These values are higher than the CIC region (0.1-0.13 wt%) reported for WPI at an a/w interface (Tamm et al., 2012). The highest C_p (1 wt%) examined in our study was significantly above the CIC levels reported by those studies. Further adsorption of proteins at concentrations above that required to form a condensed monolayer result in destabilization or collapse in ordered "2D" interfacial arrangement (Angelova, Vollhardt, & Ionov, 1996; Nikomarov, 1990). Once the monolayer has collapsed, protein molecules cannot retain highly ordered structure at the interface and begin to form multilayers (Phan, Lee, & Shin, 2016). Development of such multilayers result in the less stable interfaces. It would appear, therefore, that identifying optimal C_p is important for the formation of interfacial structures necessary for effective emulsion stability. In comparison with the slow increase in moduli at pH 7, maximum values were reached very quickly (< 250 s) for WPI at pH 4.7 (Figure 7 b). This can be attributed to the absence of electrostatic repulsion between adsorbing proteins due to net neutral charge.

However, at pH 3, interfacial moduli of WPI continued to increase with time, without a detectable plateau observed after 3600s (Figure 7 a). This is indicative of continuous conformational rearrangement over the entire experimental time frame. Interfacial films at pH 3 also showed predominantly viscous behavior (G″>G′) (Figure 7 a). Such structure may have been the result of preferential adsorption of α-lactalbumin. In order to confirm this, interfacial films were formed using pure α-lactalbumin and β-lactoglobulin proteins (Figure 9). α-lactalbumin stabilized

interfaces were also predominantly viscous in nature at pH 3 but elastic (G′>G″) at pH 7. In contrast, β-lactoglobulin films remained more solid-like (G′>G″) at both pH values and reflected the visco-elastic properties of WPI interfaces at pH 7 determined in the present study. WPI stabilized interfaces at pH 3 were similar interfacial films formed by α-lactalbumin, which suggests that it adsorbs preferentially at the o/w interface under acidic conditions. This possibility is supported by findings on the pH dependence of viscoelastic WPI films at the a/w interface (Davis et al., 2004). The conformation of α-lactalbumin transforms from it's native state into a molten globule form as the pH is decreased from 7 to acidic pH values (Dickinson, 1999). This conformational change is associated with a reduction in interfacial elasticity and viscosity (Cornec et al., 2001). In addition, WPI carries a stronger net positive charge (27.1 ± 3.2 mV) at pH 3 than a net negative charge (-21.1 ± 1.1 mV) at pH 7. Thus, electrostatic repulsion should be greater under acidic conditions (albeit with different structural conformations) and led to less extensive protein-protein interactions within the interfacial layer. As discussed earlier, WPI was more surface active at pH 3 with faster diffusion and unfolding rates, which are also indicative of greater emulsion capacity, which however, does not necessarily equate with emulsion stability. WPI, at acidic pH, seems to be less able to form strong interfacial structures, which is relevant to the (in)stability of emulsions. The relationships, however, between fundamental studies of model interfacial systems and the force and time-scales involved in high-pressure homogenization remains poorly understood. Lam and Nickerson (2015) found that WPI had higher emulsion activity and lower emulsion stability at pH 3 than pH 7, which supports the observations of this work.

Having discussed the effect of pH on the viscoelastic properties of protein adsorbed interface previously, it is now necessary to consider the effects of heat treatment as a function of pH. The elastic modulus was dominant for both HT and NHT WPI with tan δ < 1 at pH 7. In contrast, tan δ was > 1 for NHT WPI after adsorption for 3600s at pH 3 (Figure 10), indicating predominantly viscous/liquid-like character. After heating at pH 3, tan δ decreased to < 1, resulting in a more solid structure. Similar phenomena have been observed for β-lactoglobulin at an air/water interface (Kim et al., 2005). Increases in interfacial shear elasticity for HT WPI may be associated with the formation of intermolecular β-sheets during heating (Figure 2). A similar correlation was made by Renault, Pezennec, Gauthier, Vié and Desbat (2002).

The heat-induced enhancement of elastic behavior in WPI films at pH 3 is also supported by frequency sweep data (Figure 11). Buggy, McManus, Brodkorb, Carthy and Fenelon (2017) reported that WPI aggregates formed during heat-treatment can lead to a more stable emulsion. G′ values of NHT and HT WPI exhibited an exponential growth with frequency, which is in agreement with observations by Yang et al. (2020). A stronger frequency dependence can be seen for interfacial layers stabilized by NHT WPI (exponent value between 0.96 and 1.3) compared to HT WPI (exponent value between 0.31 and 0.46). The crossover point of G′ and G″ for NHT WPI occurred at higher frequency (<0.5Hz) compared to HT WPI (<0.01Hz) i.e., the relaxation time for interfacial films stabilized by NHT WPI was shorter, at pH 3, compared to HT WPI.

4. Conclusions

In this work, the effects of C_p, pH and heat treatment on the structural properties of WPI-stabilized o/w interfaces were examined. Whey proteins were more surface

active at higher $C_{p.}$ Weaker interfacial films were formed at C_p above 0.1 wt%, which was probably due to monolayer collapse and formation of protein multilayers. WPI was more surface active at pH 3, whereas interfacial films were more elastic at pH 7. Heat treatment enhanced surface activity to a lower extent at pH 3 compared to pH 7. Heated WPI formed stronger interfacial films with higher elasticity.

In considering the changes in surface charge, local structure and protein conformation, this study clarifies the influence of pH-induced preferential adsorption of individual whey proteins on the surface activity and mechanical properties of WPI adsorbed interfaces. Our investigations extend current understanding of protein structures and their associated effects on interfacial properties. These understandings of the interfacial properties of mixed protein systems, such as WPI, can contribute to better control of the complex mechanisms involved in the production and stability of food emulsions. The current study examines the mechanism for the formation and stabilization of interfacial films within the LVR. Future research is needed to characterize the viscoelastic behavior of interfacial films outside the LVR and it's correlation with mechanical destabilization processes in emulsions.

Acknowledgements

This work was supported by the Department of Agriculture, Food and Marine. Beibei Zhou was funded under the Teagasc Walsh Fellow Scheme (reference number 2017122).

References

Allain, A.-F., Paquin, P., & Subirade, M. (1999). Relationships between conformation of β-lactoglobulin in solution and gel states as revealed by attenuated total reflection

595 Fourier transform infrared spectroscopy. *International Journal of Biological*
596 *Macromolecules, 26*(5), 337-344.https://doi.org/10.1016/S0141-8130(99)00104-X
597 Álvarez Gómez, J. M., & Rodríguez Patino, J. M. (2006). Formulation Engineering of Food
598 Model Foams Containing Diglycerol Esters and β-Lactoglobulin. *Industrial &*
599 *Engineering Chemistry Research, 45*(22), 7510-
600 7519.https://doi.org/10.1021/ie060924g
601 Amagliani, L., & Schmitt, C. (2017). Globular plant protein aggregates for stabilization of food
602 foams and emulsions. *Trends in Food Science & Technology, 67*, 248-
603 259.https://doi.org/10.1016/j.tifs.2017.07.013
604 Amine, C., Dreher, J., Helgason, T., & Tadros, T. (2014). Investigation of emulsifying
605 properties and emulsion stability of plant and milk proteins using interfacial tension
606 and interfacial elasticity. *Food Hydrocolloids, 39*, 180-
607 186.https://doi.org/10.1016/j.foodhyd.2014.01.001
608 Angelova, A., Vollhardt, D., & Ionov, R. (1996). 2D−3D Transformations of Amphiphilic
609 Monolayers Influenced by Intermolecular Interactions: A Brewster Angle Microscopy
610 Study. *The Journal of Physical Chemistry, 100*(25), 10710-
611 10720.https://doi.org/10.1021/jp960417k
612 Arnebrant, T., Barton, K., & Nylander, T. (1987). Adsorption of α-lactalbumin and β-
613 lactoglobulin on metal surfaces versus temperature. *Journal of colloid and interface*
614 *science, 119*(2), 383-390.https://doi.org/10.1016/0021-9797(87)90284-0
615 Baeza, R., Carrera Sanchez, C., Pilosof, A. M. R., & Rodríguez Patino, J. M. (2005).
616 Interactions of polysaccharides with β-lactoglobulin adsorbed films at the air–water
617 interface. *Food Hydrocolloids, 19*(2), 239-
618 248.https://doi.org/10.1016/j.foodhyd.2004.06.002
619 Baldursdottir, S. G., Fullerton, M. S., Nielsen, S. H., & Jorgensen, L. (2010). Adsorption of
620 proteins at the oil/water interface--observation of protein adsorption by interfacial
621 shear stress measurements. *Colloids Surf B Biointerfaces, 79*(1), 41-
622 46.https://doi.org/10.1016/j.colsurfb.2010.03.020
623 Baldwin, A. J., Knowles, T. P., Tartaglia, G. G., Fitzpatrick, A. W., Devlin, G. L., Shammas, S.
624 L., Waudby, C. A., Mossuto, M. F., Meehan, S., Gras, S. L., Christodoulou, J.,
625 Anthony-Cahill, S. J., Barker, P. D., Vendruscolo, M., & Dobson, C. M. (2011).
626 Metastability of native proteins and the phenomenon of amyloid formation. *J Am*
627 *Chem Soc, 133*(36), 14160-14163.https://doi.org/10.1021/ja2017703
628 Barreto, M. S. C., Elzinga, E. J., & Alleoni, L. R. F. (2020). The molecular insights into
629 protein adsorption on hematite surface disclosed by in-situ ATR-FTIR/2D-COS study.
630 *Sci Rep, 10*(1), 13441.https://doi.org/10.1038/s41598-020-70201-z
631 Beverung, C. J., Radke, C. J., & Blanch, H. W. (1999). Protein adsorption at the oil/water
632 interface: characterization of adsorption kinetics by dynamic interfacial tension
633 measurements. *Biophysical Chemistry, 81*, 59-80.https://doi.org/10.1016/S0301-
634 4622(99)00082-4
635 Bos, A. M., & van Vliet, T. (2001). Interfacial rheological properties of adsorbed protein
636 layers and surfactants-a review. *Advances in Colloid and Interface Science, 91*(3),
637 437-471.https://doi.org/10.1016/S0001-8686(00)00077-4
638 Boye, J. I., Alli, I., & Ismail, A. A. (1997). Use of Differential Scanning Calorimetry and
639 Infrared Spectroscopy in the Study of Thermal and Structural Stability of α-
640 Lactalbumin. *Journal of Agricultural and Food Chemistry, 45*(4), 1116-
641 1125.https://doi.org/10.1021/jf960360z
642 Buchmann, L., Bertsch, P., Böcker, L., Krähenmann, U., Fischer, P., & Mathys, A. (2019).
643 Adsorption kinetics and foaming properties of soluble microalgae fractions at the
644 air/water interface. *Food Hydrocolloids, 97*,
645 105182.https://doi.org/10.1016/j.foodhyd.2019.105182
646 Buggy, A. K., McManus, J. J., Brodkorb, A., Carthy, N. M., & Fenelon, M. A. (2017).
647 Stabilising effect of α-lactalbumin on concentrated infant milk formula emulsions heat
648 treated pre- or post-homogenisation. *Dairy Science & Technology, 96*(6), 845-859.
649 https://doi.org/10.1007/s13594-016-0306-1

650 Cao, Y., Xiong, Y. L., Cao, Y., & True, A. D. (2018). Interfacial properties of whey protein
651 foams as influenced by preheating and phenolic binding at neutral pH. *Food*
652 *Hydrocolloids, 82*, 379-387.https://doi.org/10.1016/j.foodhyd.2018.04.020
653 Chandrapala, J., Duke, M. C., Gray, S. R., Zisu, B., Weeks, M., Palmer, M., & Vasiljevic, T.
654 (2015). Properties of acid whey as a function of pH and temperature. *Journal of Dairy*
655 *Science, 98*(7), 4352-4363.https://doi.org/10.3168/jds.2015-9435
656 Chaplin, L. C., & Lyster, R. L. J. (2009). Irreversible heat denaturation of bovine α-
657 lactalbumin. *Journal of Dairy Research, 53*(2), 249-
658 258.https://doi.org/10.1017/S0022029900024857
659 Chou, P. Y., & Fasman, G. D. (1977). β-turns in proteins. *Journal of Molecular Biology,*
660 *115*(2), 135-175.https://doi.org/10.1016/0022-2836(77)90094-8
661 Cornec, M., Cho, D., & Narsimhan, G. (1999). Adsorption dynamics of α-lactalbumin and β-
662 lactoglobulin at air-water interfaces. *Journal of colloid and interface science, 214*(2),
663 129–142.https://doi.org/10.1006/jcis.1999.6230
664 Cornec, M., Kim, D. A., & Narsimhan, G. (2001). Adsorption dynamics and interfacial
665 properties of α-lactalbumin in native and molten globule state conformation at air–
666 water interface. *Food Hydrocolloids, 15*(3), 303-313.https://doi.org/10.1016/S0268-
667 005X(01)00031-5
668 Croguennec, T., O'Kennedy, B. T., & Mehra, R. (2004). Heat-induced
669 denaturation/aggregation of β-lactoglobulin A and B: kinetics of the first intermediates
670 formed. *International Dairy Journal, 14*(5), 399-
671 409.https://doi.org/10.1016/j.idairyj.2003.09.005
672 Davis, J. P., & Foegeding, E. A. (2004). Foaming and Interfacial Properties of Polymerized
673 Whey Protein Isolate. *JOURNAL OF FOOD SCIENCE, 69*(5), C404-
674 C410.https://doi.org/10.1111/j.1365-2621.2004.tb10706.x
675 Davis, J. P., Foegeding, E. A., & Hansen, F. K. (2004). Electrostatic effects on the yield
676 stress of whey protein isolate foams. *Colloids Surf B Biointerfaces, 34*(1), 13-
677 23.https://doi.org/10.1016/j.colsurfb.2003.10.014
678 Deeth, H. C., & Bansal, N. (2019). *Whey Proteins From Milk to Medicine*: Elsevier Science.
679 Derkach, S. R., Krägel, J., & Miller, R. (2009). Methods of measuring rheological properties
680 of interfacial layers (Experimental methods of 2D rheology). *Colloid Journal, 71*(1), 1-
681 17.https://doi.org/10.1134/s1061933x09010013
682 deWit, J. N., & Klarenbeek, G. (1984). Effects of Various Heat Treatments on Structure and
683 Solubility of Whey Proteins. *Journal of Dairy Science, 67*(11), 2701-
684 2710.https://doi.org/10.3168/jds.S0022-0302(84)81628-8
685 Dickinson, E. (1999). Adsorbed protein layers at fluid interfaces: interactions, structure and
686 surface rheology. *Colloids and Surfaces B: Biointerfaces, 15*(2), 161–
687 176.https://doi.org/10.1016/S0927-7765(99)00042-9
688 Doelle, H. W., Rokem, J. S., & Berovic, M. (2009). *BIOTECHNOLOGY - Volume IV:*
689 *Fundamentals in Biotechnology*: Eolss Publishers.
690 Fox, P. F. (2008). Chapter 1 - Milk: an overview. In A. Thompson, M. Boland & H. Singh
691 (Eds.), *Milk Proteins* (pp. 1-54). San Diego: Academic Press.
692 Gao, C., Wijesinha-Bettoni, R., Wilde, P. J., Mills, E. N. C., Smith, L. J., & Mackie, A. R.
693 (2008). Surface Properties Are Highly Sensitive to Small pH Induced Changes in the
694 3-D Structure of α-Lactalbumin. *Biochemistry, 47*(6), 1659-1666.10.1021/bi700999r
695 Graham, D. E., & Phillips, M. C. (1979a). Proteins at liquid interfaces: I. Kinetics of
696 adsorption and surface denaturation. *Journal of colloid and interface science, 70*(3),
697 403-414.https://doi.org/10.1016/0021-9797(79)90048-1
698 Graham, D. E., & Phillips, M. C. (1979b). Proteins at liquid interfaces: III. Molecular
699 structures of adsorbed films. *Journal of colloid and interface science, 70*(3), 427-
700 439.https://doi.org/10.1016/0021-9797(79)90050-X
701 Graham, D. E., & Phillips, M. C. (1980). Proteins at liquid interfaces. V. Shear properties.
702 *Journal of colloid and interface science, 76*(1), 240-250.https://doi.org/10.1016/0021-
703 9797(80)90290-8

Guzey, D., McClements, D. J., & Weiss, J. (2003). Adsorption kinetics of BSA at air–sugar solution interfaces as affected by sugar type and concentration. *Food Research International, 36*(7), 649-660.https://doi.org/10.1016/S0963-9969(03)00004-8

Harwalkar, V. R. (1980). Kinetics of Thermal Denaturation of β-Lactoglobulin at pH 2.5. *Journal of Dairy Science, 63*(7), 1052-1057.https://doi.org/10.3168/jds.S0022-0302(80)83046-3

Hunt, J. A., & Dalgleish, D. G. (1994). Effect of pH on the stability and surface composition of emulsions made with whey protein isolate. *Journal of Agricultural and Food Chemistry, 42*(10), 2131-2135.https://doi.org/10.1021/jf00046a011

Jahn, T. R., & Radford, S. E. (2008). Folding versus aggregation: Polypeptide conformations on competing pathways. *Archives of Biochemistry and Biophysics, 469*(1), 100-117.https://doi.org/10.1016/j.abb.2007.05.015

Kehoe, J. J., Remondetto, G. E., Subirade, M., Morris, E. R., & Brodkorb, A. (2008). Tryptophan-Mediated Denaturation of β-Lactoglobulin A by UV Irradiation. *Journal of Agricultural and Food Chemistry, 56*(12), 4720-4725.https://doi.org/10.1021/jf0733158

Kella, N. K. D., & Kinsella, J. E. (1988). Enhanced thermodynamic stability of β-lactoglobulin at low pH. A possible mechanism. *Biochemical Journal, 255*(1), 113-118.https://doi.org/10.1042/bj2550113

Kim, D. A., Cornec, M., & Narsimhan, G. (2005). Effect of thermal treatment on interfacial properties of beta-lactoglobulin. *J Colloid Interface Sci, 285*(1), 100-109.https://doi.org/10.1016/j.jcis.2004.10.044

Kim, S. H., & Kinsella, J. E. (1985). Surface Activity of Food Proteins: Relationships Between Surface Pressure Development, Viscoelasticity of Interfacial Films and Foam Stability of Bovine Serum Albumin. *JOURNAL OF FOOD SCIENCE, 50*(6), 1526-1530.https://doi.org/10.1111/j.1365-2621.1985.tb10525.x

Krebs, M. R. H., Devlin, G. L., & Donald, A. M. (2006). Protein particulates: another generic form of protein aggregation? *Biophysical Journal, 92*(4), 1336-1342.https://doi.org/10.1529/biophysj.106.094342

Lam, R. S. H., & Nickerson, M. T. (2013). The Effect of pH and Heat Pre-Treatments on the Physicochemical and Emulsifying Properties of β-lactoglobulin. *Food Biophysics, 9*(1), 20-28.https://doi.org/10.1007/s11483-013-9313-4

Lam, R. S. H., & Nickerson, M. T. (2015). The effect of pH and temperature pre-treatments on the physicochemical and emulsifying properties of whey protein isolate. *LWT - Food Science and Technology, 60*(1), 427-434.https://doi.org/10.1016/j.lwt.2014.07.031

Langevin, D. (2014). Surface shear rheology of monolayers at the surface of water. *Advances in Colloid and Interface Science, 207*, 121-130.https://doi.org/10.1016/j.cis.2013.10.030

Lech, F. J., Delahaije, R. J. B. M., Meinders, M. B. J., Gruppen, H., & Wierenga, P. A. (2016). Identification of critical concentrations determining foam ability and stability of β-lactoglobulin. *Food Hydrocolloids, 57*, 46-54.https://doi.org/10.1016/j.foodhyd.2016.01.005

Liu, F., & Tang, C.-H. (2016). Soy glycinin as food-grade Pickering stabilizers: Part. I. Structural characteristics, emulsifying properties and adsorption/arrangement at interface. *Food Hydrocolloids, 60*, 606-619.https://doi.org/10.1016/j.foodhyd.2015.04.025

Liu, S. X. (2009). Application of Kevine-Voigt Model in Quantifying Whey Protein Adsorption on Polyethersulfone Using QCM-D. *JALA: Journal of the Association for Laboratory Automation, v. 14*(no. 4), pp. 213-220-2009 v.2014 no.2004.https://doi.org/10.1016/j.jala.2009.01.003

Lu, R., Li, W.-W., Katzir, A., Raichlin, Y., Yu, H.-Q., & Mizaikoff, B. (2015). Probing the secondary structure of bovine serum albumin during heat-induced denaturation using mid-infrared fiberoptic sensors. *Analyst, 140*(3), 765-770.https://doi.org/10.1039/C4AN01495B

759 Mahmoudi, N., Axelos, M. A. V., & Riaublanc, A. (2011). Interfacial properties of fractal and
760 spherical whey protein aggregates. *Soft Matter, 7*(17), 7643-
761 7654.https://doi.org/10.1039/C1SM05262D
762 Marinova, K. G., Basheva, E. S., Nenova, B., Temelska, M., Mirarefi, A. Y., Campbell, B., &
763 Ivanov, I. B. (2009). Physico-chemical factors controlling the foamability and foam
764 stability of milk proteins: Sodium caseinate and whey protein concentrates. *Food*
765 *Hydrocolloids, 23*(7), 1864-1876.https://doi.org/10.1016/j.foodhyd.2009.03.003
766 Martinez, M. J., & Pilosof, A. M. R. (2018). On the relationship between pH-dependent β-
767 lactoglobulin self assembly and gelation dynamics. *International Food Research*
768 *Journal, 25*(2), 676-683,
769 https://search.proquest.com/docview/2059077962?accountid=14504
770 McClements, D. J. (2004). Protein-stabilized emulsions. *Current Opinion in Colloid &*
771 *Interface Science, 9*(5), 305-313.https://doi.org/10.1016/j.cocis.2004.09.003
772 McClements, D. J., & Jafari, S. M. (2018). Improving emulsion formation, stability and
773 performance using mixed emulsifiers: A review. *Advances in Colloid and Interface*
774 *Science, 251*, 55-79.https://doi.org/10.1016/j.cis.2017.12.001
775 McGuffey, M. K., Epting, K. L., Kelly, R. M., & Foegeding, E. A. (2005). Denaturation and
776 Aggregation of Three α-Lactalbumin Preparations at Neutral pH. *Journal of*
777 *Agricultural and Food Chemistry, 53*(8), 3182-3190.https://doi.org/10.1021/jf048863p
778 Mercadante, D., Melton, Laurence D., Norris, Gillian E., Loo, Trevor S., Williams, Martin A.
779 K., Dobson, Renwick C. J., & Jameson, Geoffrey B. (2012). Bovine β-Lactoglobulin Is
780 Dimeric Under Imitative Physiological Conditions: Dissociation Equilibrium and Rate
781 Constants over the pH Range of 2.5–7.5. *Biophysical Journal, 103*(2), 303-
782 312.https://doi.org/10.1016/j.bpj.2012.05.041
783 Mulvihill, D. M., & Donovan, M. (1987). Whey Proteins and Their Thermal Denaturation - A
784 Review. *Irish Journal of Food Science and Technology, 11*(1), 43-
785 75.http://www.jstor.org/stable/25558153
786 Murphy, E. G., Fenelon, M. A., Roos, Y. H., & Hogan, S. A. (2014). Decoupling
787 macronutrient interactions during heating of model infant milk formulas. *J Agric Food*
788 *Chem, 62*(43), 10585-10593.https://doi.org/10.1021/jf503620r
789 Nikomarov, E. S. (1990). A slow collapse of a monolayer spread on an aqueous surface.
790 *Langmuir, 6*(2), 410-414.https://doi.org/10.1021/la00092a021
791 Paulsson, M., & Dejmek, P. (1992). Surface film pressure of β-lactoglobulin, α-lactalbumin
792 and bovine serum albumin at the air/water interface studied by wilhelmy plate and
793 drop volume. *Journal of colloid and interface science, 150*(2), 394-
794 403.https://doi.org/10.1016/0021-9797(92)90209-5
795 Perez, A. A., Carrara, C. R., Sánchez, C. C., Santiago, L. G., & Rodríguez Patino, J. M.
796 (2009). Interfacial dynamic properties of whey protein concentrate/polysaccharide
797 mixtures at neutral pH. *Food Hydrocolloids, 23*(5), 1253-
798 1262.https://doi.org/10.1016/j.foodhyd.2008.08.013
799 Perez, A. A., Sánchez, C. C., Patino, J. M. R., Rubiolo, A. C., & Santiago, L. G. (2010). Milk
800 whey proteins and xanthan gum interactions in solution and at the air–water interface:
801 A rheokinetic study. *Colloids and Surfaces B: Biointerfaces, 81*(1), 50-
802 57.https://doi.org/10.1016/j.colsurfb.2010.06.021
803 Phan, M., Lee, J., & Shin, K. (2016). Collapsed States of Langmuir Monolayers. *Journal of*
804 *Oleo Science, 65*.https://doi.org/10.5650/jos.ess15261
805 Renault, A., Pezennec, S., Gauthier, F., Vié, V., & Desbat, B. (2002). Surface Rheological
806 Properties of Native and S-Ovalbumin Are Correlated with the Development of an
807 Intermolecular β-Sheet Network at the Air−Water Interface. *Langmuir, 18*(18), 6887-
808 6895.https://doi.org/10.1021/la0257586
809 Rodríguez Niño, M. R., Sánchez, C. C., Ruíz-Henestrosa, V. P., & Rodríguez Patino, J. M.
810 (2005). Milk and soy protein films at the air-water interface. *Food Hydrocolloids, 19*(3),
811 417-428.https://doi.org/10.1016/j.foodhyd.2004.10.008
812 Rodríguez Patino, J. M., Miñones Conde, J., Linares, H. M., Pedroche Jiménez, J. J.,
813 Carrera Sánchez, C., Pizones, V., & Rodríguez, F. M. (2007). Interfacial and foaming

properties of enzyme-induced hydrolysis of sunflower protein isolate. *Food Hydrocolloids, 21*(5), 782-793.https://doi.org/10.1016/j.foodhyd.2006.09.002

Rodríguez Patino, J. M., Rodríguez Niño, M. R., & Sánchez, C. C. (1999). Adsorption of Whey Protein Isolate at the Oil−Water Interface as a Function of Processing Conditions: A Rheokinetic Study. *Journal of Agricultural and Food Chemistry, 47*(6), 2241−2248.https://doi.org/10.1021/jf981119i

Roth, S., Murray, B. S., & Dickinson, E. (2000). Interfacial Shear Rheology of Aged and Heat-Treated β-Lactoglobulin Films: Displacement by Nonionic Surfactant. *Journal of Agricultural and Food Chemistry, 48*(5), 1491−1497.https://doi.org/10.1021/jf990976z

Ruíz-Henestrosa, V. P., Sánchez, C. C., Escobar, M. d. M. Y., Jiménez, J. J. P., Rodríguez, F. M., & Patino, J. M. R. (2007). Interfacial and foaming characteristics of soy globulins as a function of pH and ionic strength. *Colloids and Surfaces A: Physicochemical and Engineering Aspects, 309*(1-3), 202-215.https://doi.org/10.1016/j.colsurfa.2007.01.030

Sakurai, K., & Goto, Y. (2002). Manipulating Monomer-Dimer Equilibrium of Bovine beta - Lactoglobulin by Amino Acid Substitution. *The Journal of biological chemistry, 277*, 25735-25740.https://doi.org/10.1074/jbc.M203659200

Schestkowa, H., Drusch, S., & Wagemans, A. M. (2020). FTIR analysis of β-lactoglobulin at the oil/water-interface. *Food Chemistry, 302*, 125349.https://doi.org/10.1016/j.foodchem.2019.125349

Schestkowa, H., Wollborn, T., Westphal, A., Maria Wagemans, A., Fritsching, U., & Drusch, S. (2019). Conformational state and charge determine the interfacial stabilization process of beta-lactoglobulin at preoccupied interfaces. *J Colloid Interface Sci, 536*, 300-309.https://doi.org/10.1016/j.jcis.2018.10.043

Schröder, A., Berton-Carabin, C., Venema, P., & Cornacchia, L. (2017). Interfacial properties of whey protein and whey protein hydrolysates and their influence on O/W emulsion stability. *Food Hydrocolloids, 73*, 129-140.https://doi.org/10.1016/j.foodhyd.2017.06.001

Shimizu, M., Saito, M., & Yamauchi, K. (1985). Emulsifying and Structural Properties of ß-Lactoglobulin at Different PHs. *Agricultural and Biological Chemistry, 49*(1), 189-194.https://doi.org/10.1271/bbb1961.49.189

Tamm, F., Sauer, G., Scampicchio, M., & Drusch, S. (2012). Pendant drop tensiometry for the evaluation of the foaming properties of milk-derived proteins. *Food Hydrocolloids, 27*(2), 371-377.https://doi.org/10.1016/j.foodhyd.2011.10.013

Tang, C.-H., & Shen, L. (2015). Dynamic adsorption and dilatational properties of BSA at oil/water interface: Role of conformational flexibility. *Food Hydrocolloids, 43*, 388-399.https://doi.org/10.1016/j.foodhyd.2014.06.014

Vandebril, S., Franck, A., Fuller, G. G., Moldenaers, P., & Vermant, J. (2010). A double wall-ring geometry for interfacial shear rheometry. *Rheologica Acta, 49*(2), 131-144.https://doi.org/10.1007/s00397-009-0407-3

Wahlgren, M., & Elofsson, U. (1997). Simple Models for Adsorption Kinetics and Their Correlation to the Adsorption of β-Lactoglobulin A and B. *Journal of colloid and interface science, 188*(1), 121-129.https://doi.org/10.1006/jcis.1996.4715

Wang, J. M., Xia, N., Yang, X. Q., Yin, S. W., Qi, J. R., He, X. T., Yuan, D. B., & Wang, L. J. (2012). Adsorption and dilatational rheology of heat-treated soy protein at the oil-water interface: relationship to structural properties. *J Agric Food Chem, 60*(12), 3302-3310.https://doi.org/10.1021/jf205128v

Wang, L., Xie, H., Qiao, X., Goffin, A., Hodgkinson, T., Yuan, X., Sun, K., & Fuller, G. G. (2012). Interfacial Rheology of Natural Silk Fibroin at Air/Water and Oil/Water Interfaces. *Langmuir, 28*(1), 459-467.https://doi.org/10.1021/la2041373

Ward, A. F. H., & Tordai, L. (1946). Time-Dependence of Boundary Tensions of Solutions I. The Role of Diffusion in Time-Effects. *The Journal of Chemical Physics, 14*(7), 453-461.https://doi.org/10.1063/1.1724167

Wierenga, P. A., Egmond, M. R., Voragen, A. G., & de Jongh, H. H. (2006). The adsorption and unfolding kinetics determines the folding state of proteins at the air-water

interface and thereby the equation of state. *J Colloid Interface Sci, 299*(2), 850-857.https://doi.org/10.1016/j.jcis.2006.03.016

Wijayanti, H. B., Bansal, N., & Deeth, H. C. (2014). Stability of Whey Proteins during Thermal Processing: A Review. *Comprehensive Reviews in Food Science and Food Safety, 13*(6), 1235-1251.https://doi.org/10.1111/1541-4337.12105

Wilde, P., Mackie, A., Husband, F., Gunning, P., & Morris, V. (2004). Proteins and emulsifiers at liquid interfaces. *Adv Colloid Interface Sci, 108-109*, 63-71.https://doi.org/10.1016/j.cis.2003.10.011

Won, J. Y., Gochev, G. G., Ulaganathan, V., Krägel, J., Aksenenko, E. V., Fainerman, V. B., & Miller, R. (2017). Effect of solution pH on the adsorption of BLG at the solution/tetradecane interface. *Colloids and Surfaces A: Physicochemical and Engineering Aspects, 519*, 161-167.https://doi.org/10.1016/j.colsurfa.2016.05.042

Wüstneck, R., Fainerman, V. B., Aksenenko, E. V., Kotsmar, C., Pradines, V., Krägel, J., & Miller, R. (2012). Surface dilatational behavior of β-casein at the solution/air interface at different pH values. *Colloids and Surfaces A: Physicochemical and Engineering Aspects, 404*, 17-24.https://doi.org/10.1016/j.colsurfa.2012.03.050

Yang, H., Yang, S., Kong, J., Dong, A., & Yu, S. (2015). Obtaining information about protein secondary structures in aqueous solution using Fourier transform IR spectroscopy. *Nat Protoc, 10*(3), 382-396.https://doi.org/10.1038/nprot.2015.024

Yang, J., Thielen, I., Berton-Carabin, C. C., van der Linden, E., & Sagis, L. M. C. (2020). Nonlinear interfacial rheology and atomic force microscopy of air-water interfaces stabilized by whey protein beads and their constituents. *Food Hydrocolloids, 101*.https://doi.org/10.1016/j.foodhyd.2019.105466

Yu, M., Silva, T. C., van Opstal, A., Romeijn, S., Every, H. A., Jiskoot, W., Witkamp, G.-J., & Ottens, M. (2019). The Investigation of Protein Diffusion via H-Cell Microfluidics. *Biophysical Journal, 116*(4), 595-609.https://doi.org/10.1016/j.bpj.2019.01.014

Zhai, J. l., Day, L., Aguilar, M.-I., & Wooster, T. J. (2013). Protein folding at emulsion oil/water interfaces. *Current Opinion in Colloid & Interface Science, 18*(4), 257-271.https://doi.org/10.1016/j.cocis.2013.03.002

Tables

Table 1. Amide I secondary structures (% of total) for non, heat-treated (NHT) and heat-treated (HT) WPI with bulk protein concentrations (C_p) of 1 wt% at pH 3 and pH 7.

Secondary structures	Band position (cm^{-1})[a]	NHT pH 3	HT pH 3	NHT pH 7	HT pH 7
Intermolecular β-sheet	1610-1620	1 ± 1	7 ± 1	0 ± 0	11 ± 2
Intramolecular β-sheet	1627-1630;1631-1635; 1689-1693;1694-1698	47 ± 1	35 ± 1	42 ± 2	31 ± 2
Random coil	1644-1650	9 ± 0	11 ± 2	15 ± 1	16 ± 1
α-helix	1654-1660	34 ± 1	30 ± 1	27 ± 2	20 ± 1
β-turn	1674-1676;1678-1682,1683-1687	9 ± 2	17 ± 0	17 ± 1	21 ± 1

[a] Data are from (Barreto et al., 2020; Chou & Fasman, 1977; Lu et al., 2015; Murphy et al., 2014; Yang et al., 2015).

Table 2. Characteristic dynamic parameters for diffusion of non, heat-treated (NHT) and heat-treated (HT) WPI to the o/w interface at bulk protein concentrations (C_p) 0.01-1 wt% and pH 3 and 7

pH	C_p (wt%)	Heat treatment	k_{diff}[a] ($mNm^{-1}s^{-0.5}$)	LR[b]	t_{diff}[c] (s)
3	0.01	NHT	2.17 ± 0.12	0.970 ± 0.006	35.3 ± 6.2
		HT	6.23 ± 0.65[d]	-	13.2 ± 4.0
	0.1	NHT	11.96 ± 0.98[d]	-	1.2 ± 0.8
		HT	-	-	<0.7
	1	NHT	-	-	<0.7
		HT	-	-	<0.7
7	0.01	NHT	1.61 ± 0.16	0.955 ± 0.038	47.8 ± 5.1
		HT	8.30 ± 1.07[d]	-	2.6 ± 1.8
	0.1	NHT	10.10 ± 0.36[d]	-	3.8 ± 0.4
		HT	-	-	<0.7
	1	NHT	11.71 ± 0.54[d]	-	<0.7
		HT	-	-	<0.7

[a] The slope of the linear region in the π-t1/2 plot is taken as the rate of initial diffusion-controlled migration.
[b] Linear regression coefficient.
[c] Period during which diffusion controls the kinetics of adsorption of WPI at the o/w interface.
[d] indication of the diffusion of WPI to the o/w interface.
Each datum was the average of triplicate measurements on separate samples.

Table 3. Characteristic dynamic parameters for the unfolding and rearrangement of the non, heat-treated (NHT) and heat-treated (HT) WPI at bulk protein concentrations (C_p) of 0.01-1 wt% and pH 3 and 7

pH	C_p (wt%)	Heat treatment	k_u[a] $\times 10^4$ (s^{-1})	LR[b]	k_r[c] $\times 10^4$ (s^{-1})	LR[b]
3	0.01	NHT	2.72 ± 0.06	0.985 ± 0.008	26.35 ± 0.29	0.944 ± 0.032
		HT	2.28 ± 0.09	0.921± 0.029	5.24 ± 0.88	0.915 ± 0.01
	0.1	NHT	3.20 ± 0.30	0.948 ± 0.016	24.88 ± 0.83	0.950 ± 0.027
		HT	1.82 ± 0.43	0.922 ± 0.035	8.60 ± 0.71	0.917 ± 0.028
	1	NHT	4.15 ± 0.5	0.91 ± 0.002	13.26 ± 0.62	0.915 ± 0.012
		HT	1.59 ± 0.37	0.918 ± 0.028	10.91 ± 0.57	0.948 ± 0.027
7	0.01	NHT	2.37 ± 0.11	0.981 ± 0.005	19.37 ± 0.27	0.916 ± 0.052
		HT	2.04 ± 0.11	0.972 ± 0.018	6.80 ± 0.26	0.920 ± 0.019
	0.1	NHT	2.51 ± 0.01	0.959 ± 0.014	25.12 ± 0.85	0.913 ± 0.012
		HT	2.34 ± 0.14	0.987 ± 0.008	18.11 ± 0.37	0.934 ± 0.021
	1	NHT	2.77 ± 0.16	0.932 ± 0.017	9.78 ± 1.02	0.935 ± 0.028
		HT	2.05 ± 0.08	0.959 ± 0.009	6.90 ± 0.14	0.924 ± 0.021

[a] The first slop of plot of ln[(π15000 – πt) / (π15000 – π0)] as a function of time is taken to correspond to a first-order rate constant of penetration and unfolding.
[b] Linear regression coefficient.
[c] The second slop of plot of ln[(π15000 – πt) / (π15000 – π0)] as a function of time is taken as a first-order rate constant of rearrangement.
Each datum was the average of triplicate measurements on separate samples.

Figures

Figure 1. Volume-weighted particle size for non, heat-treated (NHT) and heat-treated (HT) WPI solutions with bulk protein concentrations (C_p) of 1 wt% at pH 3 and 7

Figure 2. Second derivative FTIR spectra of non, heat-treated (NHT) and heat-treated (HT) WPI with bulk protein concentrations (C_p) of 1 wt% at pH 3 and pH 7

Figure 3. Curve-fitted, inverted second-derivative amide I spectra for WPI with bulk protein concentrations (C_p) of 1 wt%. (a) non, heat-treated (NHT) WPI at pH 3, (b) heat-treated (HT) WPI at pH 3, (c) non, heat-treated (NHT) WPI at pH 3 and (d) heat-treated (NHT) at pH 7. Second-derivative spectra were inverted by factoring by −1.

Figure 4. Interfacial pressure (π) as a function of time ($s^{1/2}$) for non, heat-treated (NHT) and heat-treated (HT) WPI stabilised o/w interfaces, formed with bulk protein concentrations (C_p) of 0.01-1 wt%. (a) pH 3 and (b) pH 7. The separated columns of symbols to the right of the data are for the purposes of clarification.

Figure 5. Interfacial pressure values after 15,000s (π15,000) as a function of bulk protein concentrations (C_p) for non, heat-treated (NHT) and heat-treated (HT) WPI at the o/w interface. (a) pH 3 and (b) pH 7

Figure 6. Representative fit of first-order rate constants of unfolding (k_u) and rearrangement (k_r) for WPI at o/w interface (pH 7)

Figure 7. The development of the interfacial elastic modulus G′ and viscous modulus G″ as function of time for non, heat-treated (NHT) WPI at o/w interfaces at (a) pH 3, (b) pH 4.7 and (c) pH 7. The separated columns of symbols to the right of the data are for the purposes of clarification.

Figure 8. Interfacial elastic modulus G′ and viscous modulus G″ as function of strain for non, heat-treated (NHT) WPI with bulk protein concentrations (C_p) of 0.01-1 wt% at o/w interface, pH 7. The separated columns of symbols to the right of the data are for the purposes of clarification.

Figure 9. Development of interfacial elastic moduli G′ and G″ as function of time for α-lactalbumin, β-lactoglobulin and non, heat-treated (NHT) WPI at o/w interfaces. (a) pH 3 and (b) pH 7. The separated columns of symbols to the right of the data are for the purposes of clarification.

Figure 10. Tan δ after 3600s adsorption as a function of protein bulk concentration for non, heat-treated (NHT) and heat-treated (HT) WPI at oil/water interfaces. (a) pH 3 and (b) pH 7

Figure 11. Interfacial elastic modulus G′ and viscous modulus G″ as function of frequency for (a) non, heat-treated (NHT) and (b) heat-treated (HT) WPI with bulk protein concentrations (C_p) of 0.01-1 wt% at o/w interfaces, pH 3. The separated columns of symbols to the right of the data are for the purposes of clarification.

Figure 1

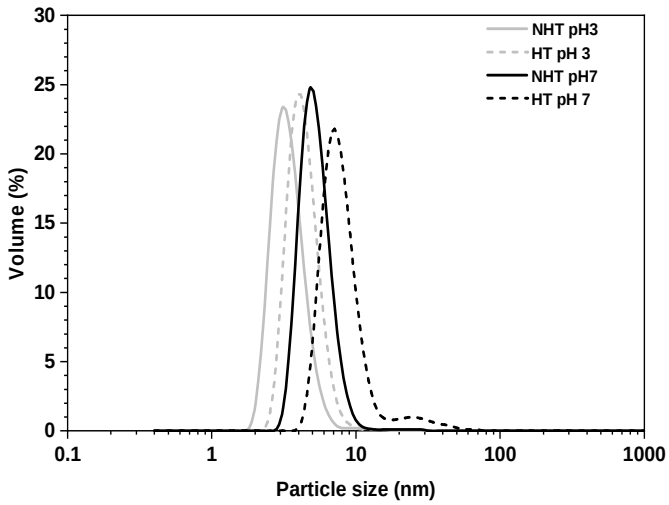

Figure 2

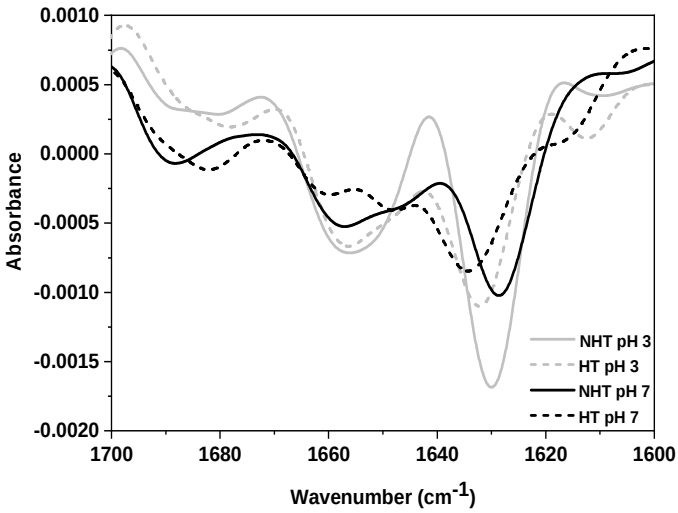

Figure 3

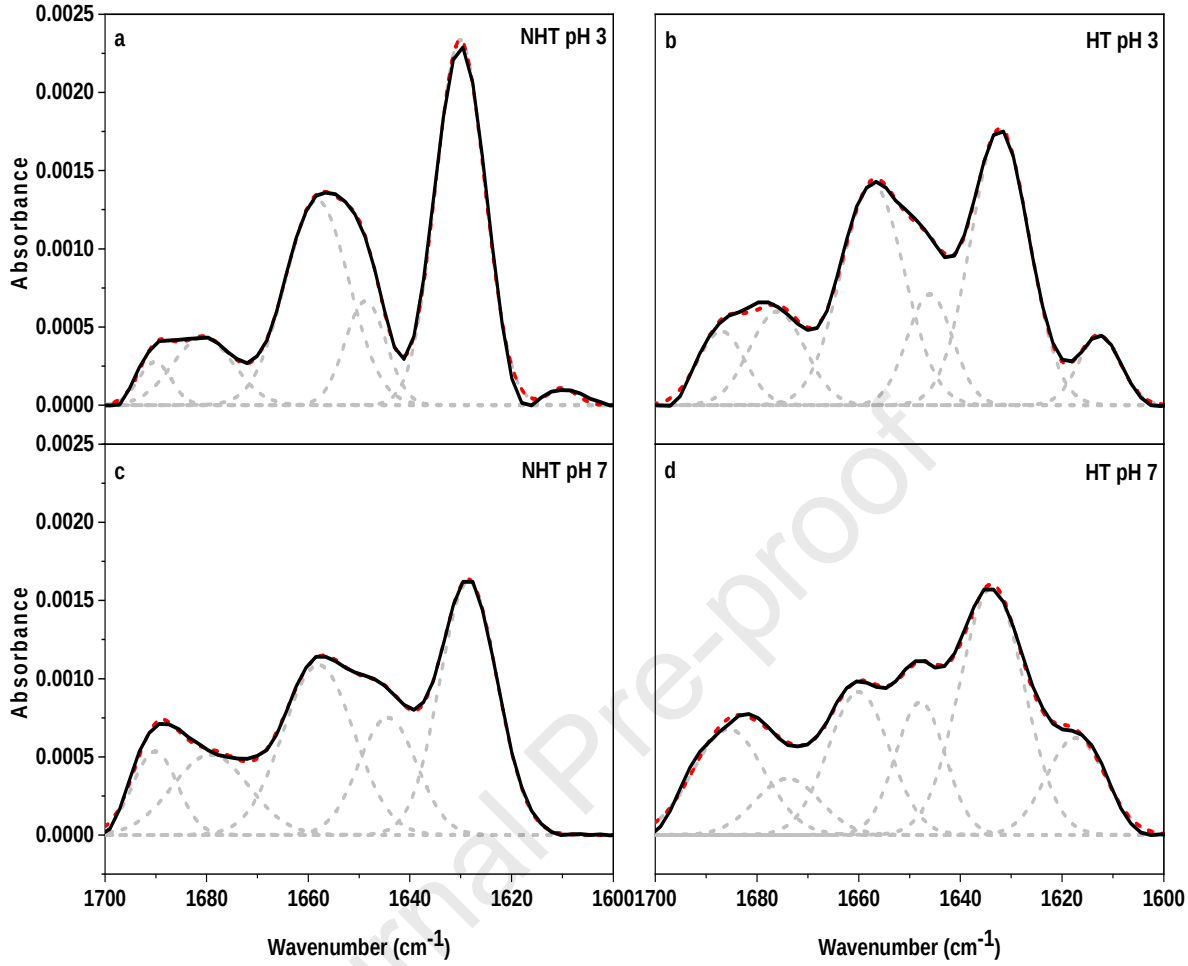

Figure 4

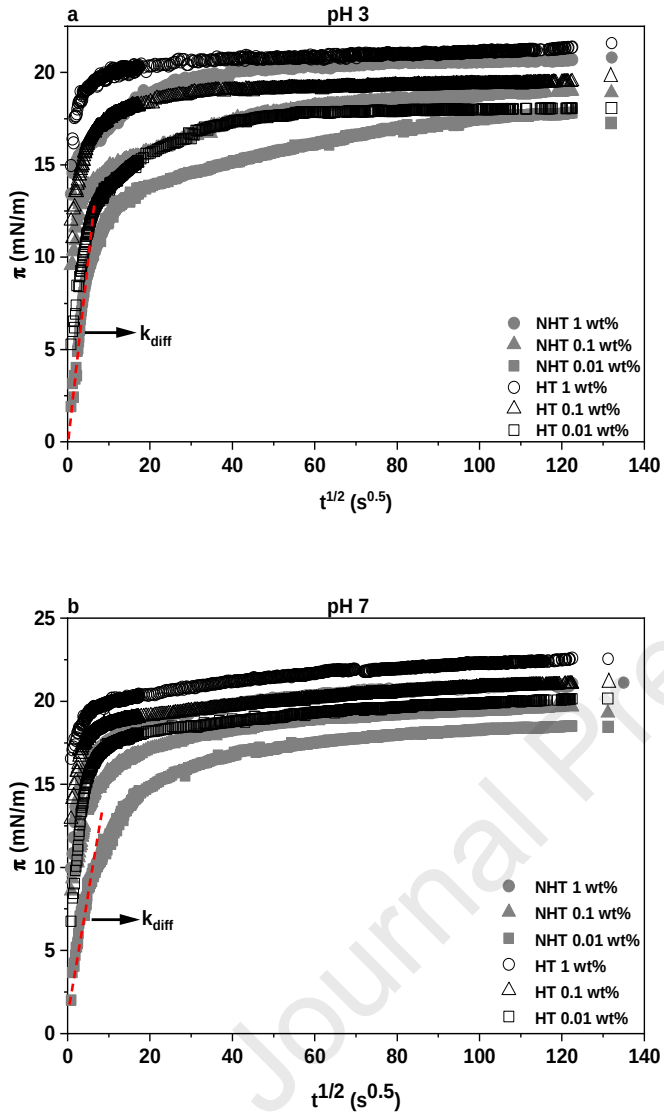

Figure 5

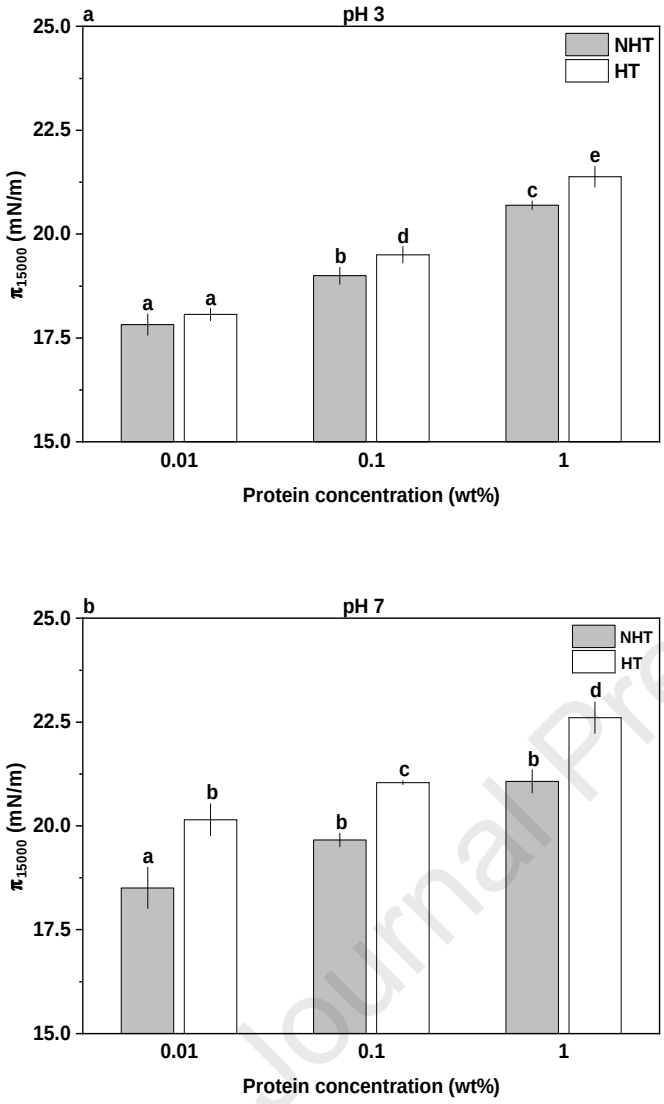

Figure 6

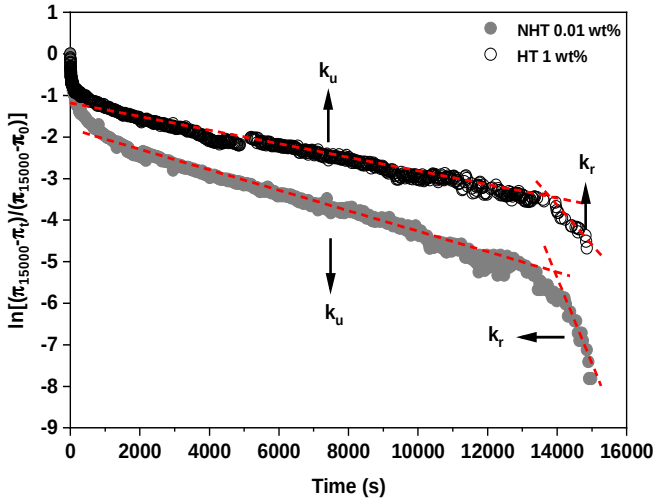

Figure 7

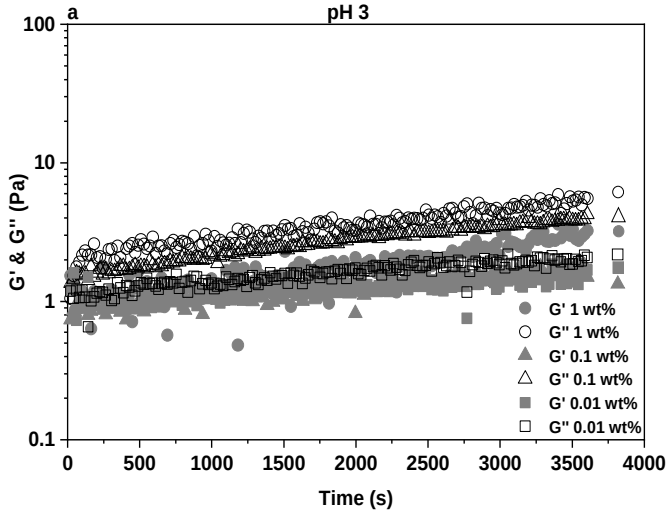

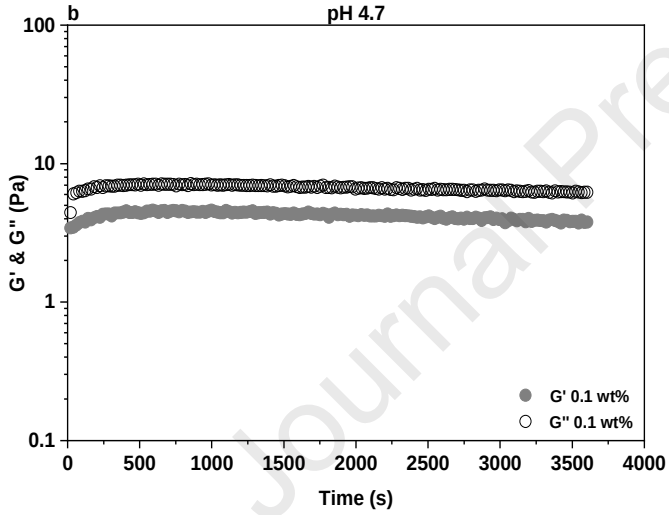

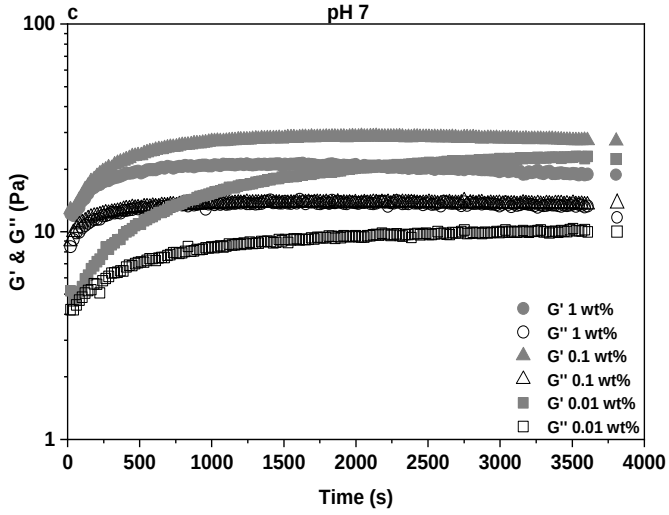

Figure 8

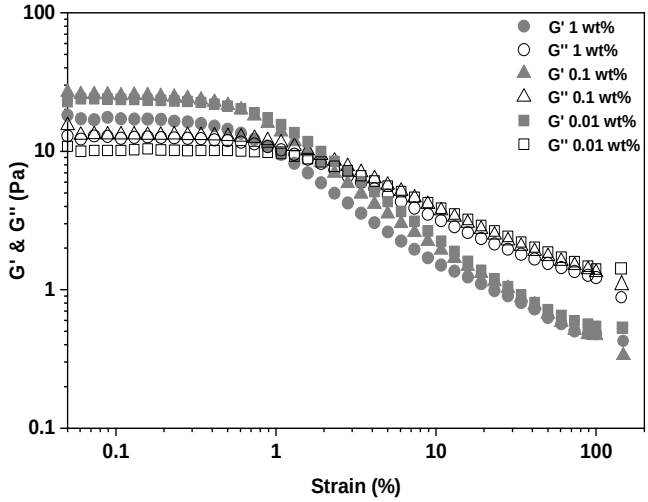

Figure 9

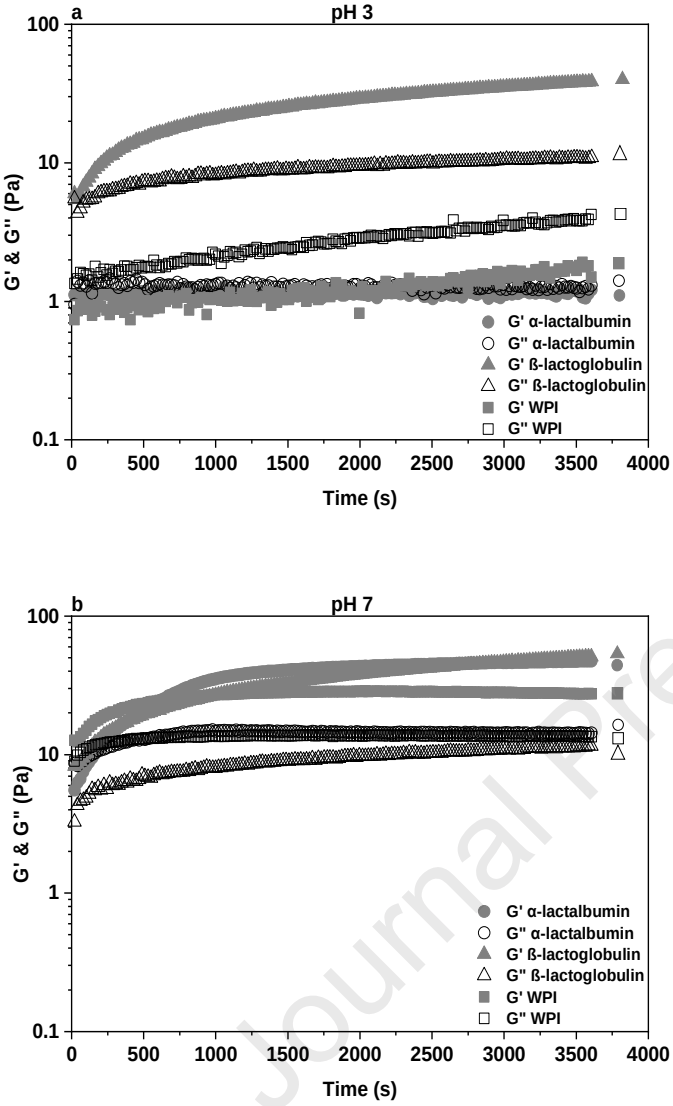

Figure 10

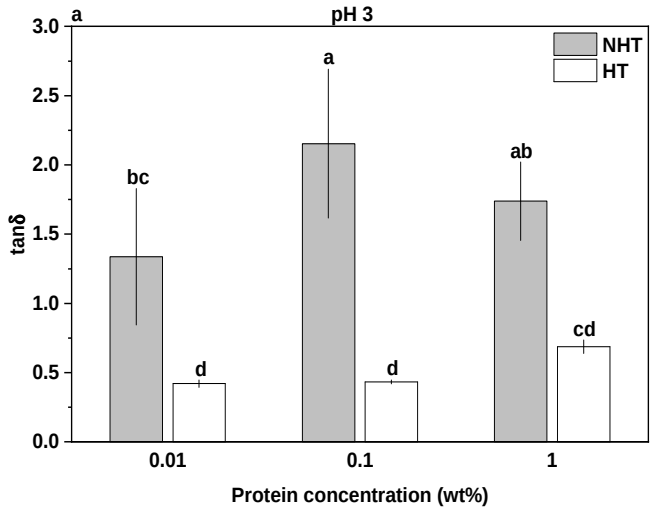

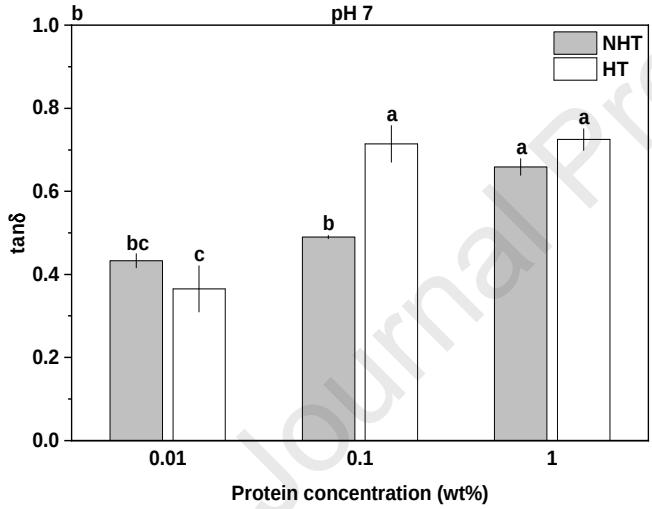

Figure 11

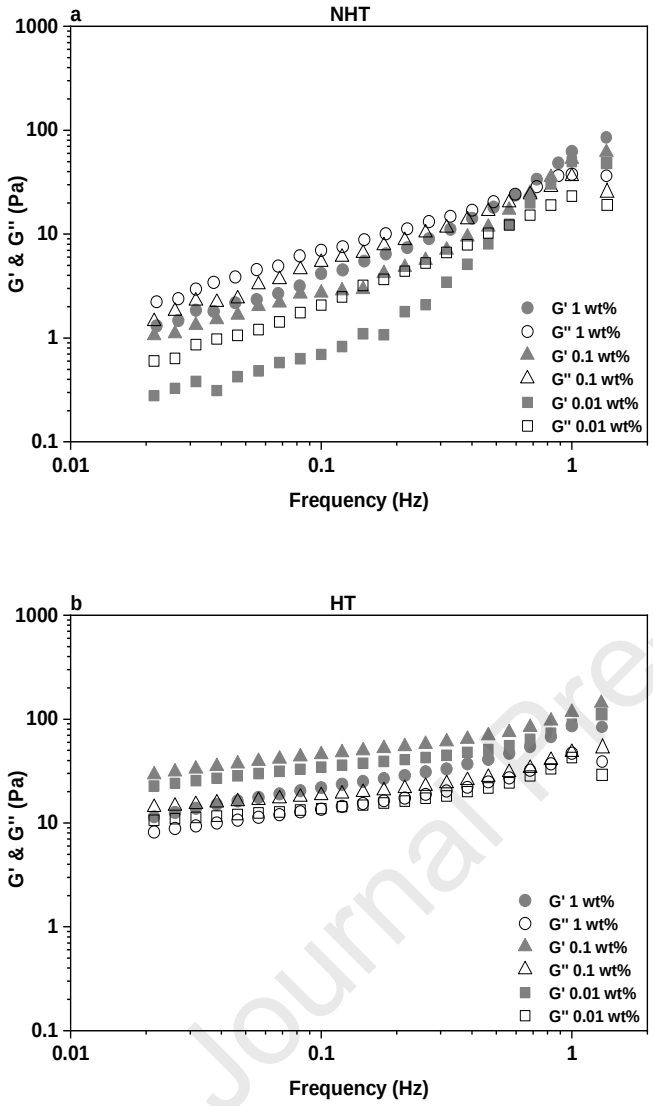

Highlights

- Conformational state of individual whey protein species at acidic pH facilitated faster adsorption.
- Greater heat stability of whey proteins at low pH resulted in less enhanced interfacial activity by heat treatment.
- At protein concentration above that required to form a condensed monolayer led to weaker interfacial films.
- pH induced preferential adsorption and protein surface charge had considerable influences on the mechanical properties of interfacial films.
- The enhancement of intermolecular interactions following heat treatment led to more solid-like interfacial structure.

Declaration of interests

✓The authors declare that they have no known competing financial interests or personal relationships that could have appeared to influence the work reported in this paper.

☐The authors declare the following financial interests/personal relationships which may be considered as potential competing interests: